ROME 2008
LEVERAGING TECHNOLOGY

P048

A 3D Parsimonious Finite-volume Frequency-domain Method for Elastic Wave Modelling

V. Etienne* (Geosciences Azur), R. Brossier (Geosciences Azur), J. Virieux (Geosciences Azur) & S. Operto (Geosciences Azur)

SUMMARY

We present the finite-volume (FV or P0 Galerkin Discontinuous) formulation applied to the 3D visco-elastic wave equation in the frequency domain. This work is motivated within the framework of global offset seismic imaging by full waveform inversion. Concerning the direct problem, the FV formulation leads to the resolution of a large and sparse system of linear equations. This system can be solved with a direct solver particuraly suitable to tomographic applications since only one matrix factorization is performed per frequency for all the right hand terms (i.e. the sources). On the other hand, direct solvers require large amount of RAM and therefore restrict the possible field of realistic applications. The memory complexity of the proposed method implies reduced size models spanning over several wavelengths. In order to push back this limitation, the use of a higher order of interpolation, as Pk Galerkin Discontinuous, should decrease the discretization step allowing coarser meshes leading to a possible managing situation. Furthermore, the use of a domain decomposition method might reduce significantly the memory requirements of the FV frequency domain approach.

Introduction

The simulation of wave propagation in complex medium has been efficiently approached with finite-difference (FD) methods and applied with success to numerous physical problems since the past decades. Nevertheless, FD methods suffer from some critical issues inherent to the underlying Cartesian grid such as parasite reflexions in case of boundaries with complex topography. Therefore and thanks to the ever increasing computation power, others methods have focused a lot of interests. Concerning the 3D elastic seismic wave equation, we can mention the finite-volume (FV) method (Dormy and Tarantola, 1995) and more recently the Galerkin Discontinuous method (Dumbser and Käser, 2006). These approaches offer the possibility to use meshes fitting almost perfectly complex topographies thus overcoming the staircase pattern relative to FD methods.
We present here the FV formulation applied to the 3D visco-elastic wave equation in the frequency domain. This work is motivated within the framework of global offset seismic imaging by full waveform inversion (FWI) which has been proved to be efficient and stable in the frequency domain (Pratt *et al.* , 1998). Concerning the direct problem, the FV formulation leads to the resolution of a large and sparse system of linear equations. This system can either be solved with a direct solver or an iterative solver (or even an hybrid approach). Direct solvers are particuraly suitable to tomographic applications since only one matrix factorization is performed per frequency for all the right hand terms (i.e. the sources) while the system has to be solved for each source in the case of iterative solvers. On the other hand, direct solvers require large amount of RAM and therefore restrict the possible field of realistic applications. In the following, we address the feasability of modelling 3D elastic wave in complex geological medium with FV method in the frequency domain with the direct solver option. After introducing the FV formulation we present some insights regarding the numerical cost versus the size of the studied model. Finaly, we discuss the perspectives of the frequency domain formulation.

Finite Volume Formulation

The elastodynamic system (1) expressed in the frequency domain for an isotropic medium is a first order hyperbolic system linking the components of the velocity vector $\vec{v} = (v_x, v_y, v_z)^t$ and the components of the stress tensor $\vec{\sigma} = (\sigma_{xx}, \sigma_{yy}, \sigma_{zz}, \sigma_{xy}, \sigma_{xz}, \sigma_{yz})^t$.

$$
\begin{aligned}
-i\omega v_x(\mathbf{x},\omega) &= \frac{1}{\rho(\mathbf{x})}\{s_x(\mathbf{x})\frac{\partial \sigma_{xx}(\mathbf{x},\omega)}{\partial x} + s_y(\mathbf{x})\frac{\partial \sigma_{xy}(\mathbf{x},\omega)}{\partial y} + s_z(\mathbf{x})\frac{\partial \sigma_{xz}(\mathbf{x},\omega)}{\partial z} + f_x(\mathbf{x},\omega)\}\\
-i\omega v_y(\mathbf{x},\omega) &= \frac{1}{\rho(\mathbf{x})}\{s_x(\mathbf{x})\frac{\partial \sigma_{xy}(\mathbf{x},\omega)}{\partial x} + s_y(\mathbf{x})\frac{\partial \sigma_{yy}(\mathbf{x},\omega)}{\partial y} + s_z(\mathbf{x})\frac{\partial \sigma_{yz}(\mathbf{x},\omega)}{\partial z} + f_y(\mathbf{x},\omega)\}\\
-i\omega v_z(\mathbf{x},\omega) &= \frac{1}{\rho(\mathbf{x})}\{s_x(\mathbf{x})\frac{\partial \sigma_{xz}(\mathbf{x},\omega)}{\partial x} + s_y(\mathbf{x})\frac{\partial \sigma_{yz}(\mathbf{x},\omega)}{\partial y} + s_z(\mathbf{x})\frac{\partial \sigma_{zz}(\mathbf{x},\omega)}{\partial z} + f_z(\mathbf{x},\omega)\}\\
-i\omega \sigma_{xx}(\mathbf{x},\omega) &= (\lambda(\mathbf{x}) + 2\mu(\mathbf{x}))s'_x(\mathbf{x})\frac{\partial v_x(\mathbf{x},\omega)}{\partial x} + \lambda(\mathbf{x})\{s'_y(\mathbf{x})\frac{\partial v_y(\mathbf{x},\omega)}{\partial y} + s'_z(\mathbf{x})\frac{\partial v_z(\mathbf{x},\omega)}{\partial z}\}\\
-i\omega \sigma_{yy}(\mathbf{x},\omega) &= (\lambda(\mathbf{x}) + 2\mu(\mathbf{x}))s'_y(\mathbf{x})\frac{\partial v_y(\mathbf{x},\omega)}{\partial y} + \lambda(\mathbf{x})\{s'_x(\mathbf{x})\frac{\partial v_x(\mathbf{x},\omega)}{\partial x} + s'_z(\mathbf{x})\frac{\partial v_z(\mathbf{x},\omega)}{\partial z}\}\\
-i\omega \sigma_{zz}(\mathbf{x},\omega) &= (\lambda(\mathbf{x}) + 2\mu(\mathbf{x}))s'_z(\mathbf{x})\frac{\partial v_z(\mathbf{x},\omega)}{\partial z} + \lambda(\mathbf{x})\{s'_x(\mathbf{x})\frac{\partial v_x(\mathbf{x},\omega)}{\partial x} + s'_y(\mathbf{x})\frac{\partial v_y(\mathbf{x},\omega)}{\partial y}\}\\
-i\omega \sigma_{xy}(\mathbf{x},\omega) &= \mu(\mathbf{x})\{s'_y(\mathbf{x})\frac{\partial v_x(\mathbf{x},\omega)}{\partial y} + s'_x(\mathbf{x})\frac{\partial v_y(\mathbf{x},\omega)}{\partial x}\}\\
-i\omega \sigma_{xz}(\mathbf{x},\omega) &= \mu(\mathbf{x})\{s'_z(\mathbf{x})\frac{\partial v_x(\mathbf{x},\omega)}{\partial z} + s'_x(\mathbf{x})\frac{\partial v_z(\mathbf{x},\omega)}{\partial x}\}\\
-i\omega \sigma_{yz}(\mathbf{x},\omega) &= \mu(\mathbf{x})\{s'_z(\mathbf{x})\frac{\partial v_y(\mathbf{x},\omega)}{\partial z} + s'_y(\mathbf{x})\frac{\partial v_z(\mathbf{x},\omega)}{\partial y}\}
\end{aligned}
\tag{1}
$$

The density of the medium is noted with ρ while λ and μ are the Lamé coefficients. In this system appear the external force $\vec{f} = (f_x, f_y, f_z)^t$. Moreover, we have introduced the Perfectly Matched Layer conditions (Berenger, 1994) to avoid undesirable reflexions at the borders of the numerical model. The damping coefficients s_α and s'_α ($\forall \alpha \in \{x, y, z\}$) are equals to 1 in the medium and carry complex values in the surrounding PML layers. The finite-volume can be seen as an interpolation of order 0, noted P0, in the Galerkin Discontinuous formulation. It relies on a volume integration of the system (1) expressed with a divergence form (2) via the introduction of functions $\vec{F}(\vec{\sigma})$ and $\vec{G}(\vec{v})$.

$$\begin{aligned} -i\omega\rho\vec{v} &= \overrightarrow{div(\vec{F}(\vec{\sigma}))} + \vec{f} \\ -i\omega\Lambda_0\vec{\sigma} &= \overrightarrow{div(\vec{G}(\vec{v}))} \end{aligned} \tag{2}$$

Λ_0 is a matrix containing the physical properties of the medium. The volume integration of (2) is performed over a control cell K_i with the P0 Galerkin Discontinuous assumption that $\vec{\sigma}$ and $\vec{v}$ are constant in the whole cell volume. With these considerations we obtain the system (3),

$$\begin{aligned} -i\omega\rho_i V_i\vec{v_i} &= \sum_{j\in K_i} S_{ij}F_{ij} + V_i\vec{f_i} \\ -i\omega\Lambda_{0_i} V_i\vec{\sigma_i} &= \sum_{j\in K_i} S_{ij}G_{ij}, \end{aligned} \tag{3}$$

with $V_i = \int_{K_i} dv$ the volume of cell K_i, $j \epsilon K_i$ are the different cells j having a common interface with cell i and S_{ij} the surface of the interface between cells i and j. $S_{ij}F_{ij}$ and $S_{ij}G_{ij}$ are respectively approximations of numerical fluxes of $\vec{\sigma}$ and $\vec{v}$ through the surface S_{ij}. For the estimation of these numerical fluxes, centered flux scheme is used for its good behavior against numerical dispersion (BenJemaa *et al.* , 2007) while keeping conserved a discrete energy. System (3) becomes the following one,

$$\begin{aligned} \omega^2\rho_i V_i\vec{v_i} &= \frac{i\omega}{2}\sum_{j\in K_i} \vec{F}(\vec{\sigma_j})\cdot\vec{n}_{ij}S_{ij} + i\omega V_i\vec{f_i} \\ \omega^2\Lambda_{0_i} V_i\vec{\sigma_i} &= \frac{i\omega}{2}\sum_{j\in K_i} \vec{G}(\vec{v_j})\cdot\vec{n}_{ij}S_{ij}, \end{aligned} \tag{4}$$

with $\vec{n}_{ij}$ the normal vector to the interface between cells i and j. Finally, we adopt the parsinonious formulation in order to keep only velocity unknowns, as shown in the following expression

$$\omega^2\rho_i V_i\vec{v_i} = \frac{i\omega}{2}\sum_{j\in K_i} S_{ij}\vec{F}\Big(\frac{i\Lambda_{0_j}^{-1}}{2\omega V_j}\sum_{k\in K_j} S_{jk}\vec{G}(\vec{v_k})\cdot\vec{n}_{jk}\Big)\cdot\vec{n}_{ij} + i\omega V_i\vec{f_i}, \tag{5}$$

where $k \epsilon K_j$ are the neighbour cells k of cell j. In the expression above, only unkwowns relative to cells i and k are present, meaning that the adopted stencil takes into account the neighbours of neighbours in the manner of a red/black scheme (Brossier *et al.* , 2007). Equation (5) can be written as a linear system $\mathcal{A}\mathcal{X} = \mathcal{B}$ where $\mathcal{A}$ is the impedance matrix, $\mathcal{X}$ the velocity unknown vector $(v_{x_1}, v_{y_1}, v_{z_1} ... v_{x_n}, v_{y_n}, v_{z_n})^t$ with n the number of cells in the model. $\mathcal{B}$ is the source term $(f_{x_1}, f_{y_1}, f_{z_1} ... f_{x_n}, f_{y_n}, f_{z_n})^t$. For the space discretization, we adopt a tetrahedral mesh with a pattern of 5 tetrahedrons embeded in an elementary cube (figure 1.a) . With such mesh, $\mathcal{A}$ is band diagonal and contains 39 non null coefficients per row (figure 1.b). If we consider a mesh with N cubes along the 3 directions, the number of cells is $5N^3$, the rank of the matrix is $15N^3$ and its bandwidth equals $30N^2$. The following section estimates the numerical cost to solve this linear system with a direct approach.

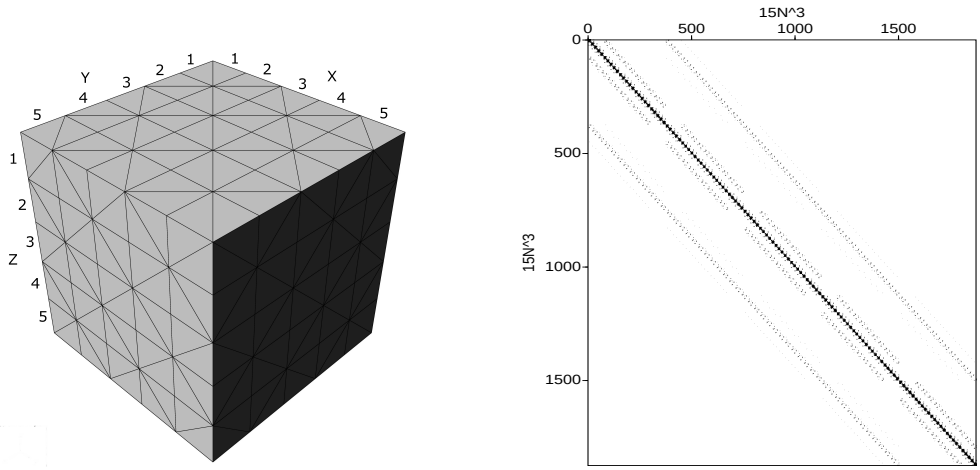

Figure 1: (a) Example of mesh with 5 elementary cubes along the 3 directions. Each cube contains 5 tetrahedrons (4 located at non contiguous corners of the cube and 1 inside the cube). (b) Impedance matrix relative to the mesh illustrated in (a). The rank of the matrix is 1875 and its bandwidth equals 750.

Numerical cost

The resolution of the linear system is done with the massively parallel direct solver MUMPS (Amestoy *et al.* , 2006) via a LU factorization. The amount of memory necessary to store the LU factors corresponds to the filling of the band diagonal of $\mathcal{A}$ and thus is $\mathcal{O}(N^5)$. Thanks to a reordering of the matrix coefficients, the memory complexity of the factorization should theorically be reduced to $\mathcal{O}(N^4)$ (Ashcraft and Liu, 1998). The figure 2.a presents the effective amount of memory allocated during computations for different model sizes. These computations have been performed on a PC cluster with 192 processors and total of 400 GBytes RAM. With this configuration, the memory required with N=55 is 352 GBytes and the elapsed time of computation is about 2 hours for one source. The velocity field for one frequency is illustrated in figure 2.b in the case of a punctual force along the x axis located in the middle of the model. In this example, the size of the model is 900 meters which represents approximately twice the longuest propagated wavelength (i.e. $\lambda_P = 400m$). Discretization is done with 10 cubes per shortest wavelength (with $\lambda_S = 200m$ cube size is 20m). The average ratio between the number of LU factors and N^4 fluctuates between 1000 and 1700 when N is increasing (figure 2.b). These results have to be compared with the numerical cost of the 3D acoustic FDFD approach where same ratio equals 35 with a cubic grid (Operto *et al.* , 2007). For similar numerical cubic models, the factor between elastic and acoustic modelling in terms of RAM needs is about 50.

Conclusions and future works

The memory complexity of the proposed method implies reduced size models spanning over several wavelengths. The future works will concern the possible options to push back this limitation. The use of a higher order of interpolation, as Pk Galerkin Discontinuous, should increase the number of coefficients of the impedance matrix and decrease the discretization step allowing coarser meshes leading to a possible managing situation. Using a domain decomposition method (Saad, 2003) might reduce significantly the memory requirements of the frequency domain approach.

Acknowledgments

This work was carried out in the frame of the SEISCOPE consortium sponsored by BP, CGG VERITAS, EXXON, SHELL and TOTAL. The computations were performed on the cluster of the Mesocentre SIGAMM (Observatoire de la Côte d'Azur).

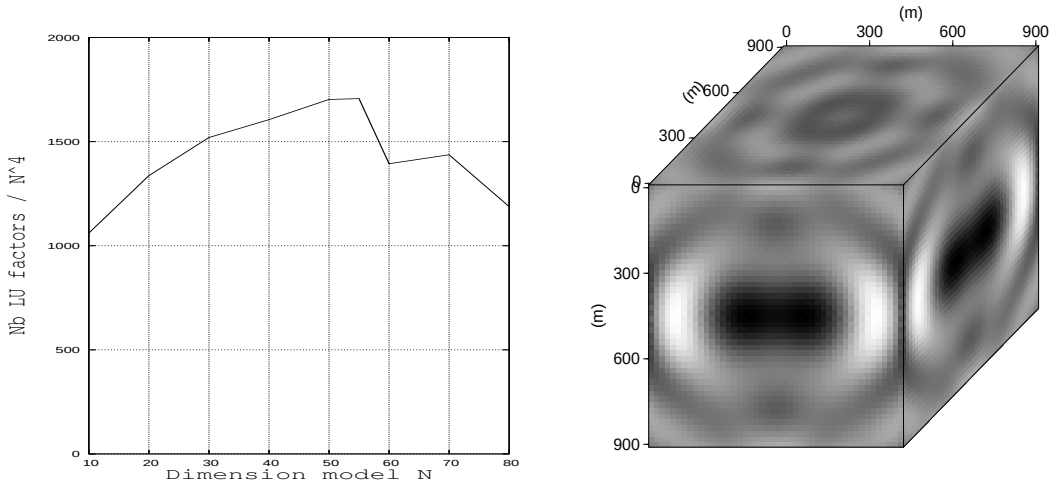

Figure 2: (a) Ratio between the number of LU factors and N^4 for different model sizes with MUMPS solver. (b) View of the component v_x (real part) for N=55 at 10 Hz after removing the PML layers for an homogeneous isotropic medium with $V_P = 4km.s^{-1}$ and $V_S = 2km.s^{-1}$. Discretization is done with 10 cubes per the shortest wavelength to provide a good accuracy.

References

Amestoy, P. R., Guermouche, A., L'Excellent, J. Y., and Pralet, S. [2006] Hybrid scheduling for the parallel solution of linear systems. *Parallel computing* 32, 136–156.

Ashcraft, Cleve, and Liu, Joseph W. H. [1998] Robust ordering of sparse matrices using multisection. *SIAM Journal on Matrix Analysis and Applications* 19(3), 816–832.

BenJemaa, M., Glinsky-Olivier, N., Cruz-Atienza, V. M., Virieux, J., and Piperno, S. [2007] Dynamic non-planar crack rupture by a finite volume method. *Geophysical Journal International* 171, 271–285.

Berenger, J-P. [1994] A perfectly matched layer for absorption of electromagnetic waves. *Journal of Computational Physics* 114, 185–200.

Brossier, R., Virieux, J., and Operto, S. [2007] Finite volume method for 2D PSV elastodynamic equations in frequency domain with velocity parsimonious formulation. *In: Expanded abstracts* Soc. Expl. Geophys.

Dormy, E., and Tarantola, A. [1995] Numerical simulation of elastic wave propagation using a finite volume method. *Journal of Geophysical Research* 100, 2123–2133.

Dumbser, M., and Käser, M. [2006] An arbiratary high-order discontinuous Galerkin method for elastic waves on unstructured meshes - II. The three-dimentional isotropic case. *Geophysical Journal International* 196(2), 319–336.

Operto, S., Virieux, J., Amestoy, P., L'Excellent, J-Y., Giraud, L., and Ben-Hadj-Ali, H. [2007] 3D finite-difference frequency-domain modeling of visco-acoustic wave propagation using a massively parallel direct solver: A feasibility study. *Geophysics* 72, 195–211.

Pratt, R. G., Shin, C., and Hicks, G. J. [1998] Gauss-newton and full newton methods in frequency-space seismic waveform inversion. *Geophysical Journal International* 133, 341–362.

Saad, Y. [2003] *Iterative methods for sparse linear systems* Vol. second edition Philadelphia: SIAM.